

Polarization and Variation of Near-IR Light from *Fermi*/LAT γ -ray Sources

M. Fujiwara¹, Y. Matsuoka¹, and N. Ienaka²

ABSTRACT

We present the results of our follow-up observation program of γ -ray sources detected by the Large Area Telescope (LAT) on board the *Fermi Gamma-ray Space Telescope*. 26 blazars and 39 sources unidentified at other wavelengths were targeted at IRSF 1.4 m telescope equipped with the SIRIUS/SIRPOL imager and polarimeter. H -band magnitudes of the blazars at the epoch of 2010 Dec – 2011 Feb are presented, which reveal clear flux variation since the Two Micron All Sky Survey observations and can be useful data for variation analyses of these objects in longer periods. We also find that nearly half of the γ -ray blazars are highly ($>10\%$) polarized in near-infrared wavelengths. Combining the polarization and variation properties, most ($\sim 90\%$) of the blazars are clearly distinguished from all other types of objects at high Galactic latitudes. On the other hand, we find only one highly polarized and/or variable object in the fields of unidentified sources. This object is a counterpart of the optical variable source PQV1 J131553.00–073302.0 and the radio source NVSS J131552–073301, and is a promising candidate of new γ -ray blazars. From the measured polarization and variation statistics, we conclude that most of the *Fermi*/LAT unidentified sources are not likely similar types of objects to the known γ -ray blazars.

Subject headings: BL Lacertae objects: general — gamma rays: galaxies — galaxies: active — galaxies: jets — polarization — quasars: general

1. Introduction

A new era of blazar studies has arrived with the advent of the *Fermi Gamma-ray Space Telescope* (*Fermi*). *Fermi* has been carrying out an all-sky survey with its main instrument Large Area Telescope (LAT) since the science mission phase started in 2008. The first *Fermi*-LAT catalog (1FGL; Abdo et al. 2010a) lists 1451 γ -ray detections, in which 821 sources are associated (or identified) with objects found at other wavelengths. The majority of the associated objects are active galactic nuclei (AGNs) dominated by blazars, while other extragalactic sources as well as Galactic objects such as pulsars and supernova remnants make smaller contributions. The remaining 630

sources are left unidentified in 1FGL.

Blazars are considered to be AGNs whose jets are aligned with the observer’s line-of-sight. Emission from the relativistically boosted jets dominates observed flux, resulting in two broad peaks in the spectral energy distribution (SED); one at radio to X-rays arising from synchrotron emission of accelerated, high-energy particles, and another at X-ray to γ -ray arising from the inverse Compton scattering of the lower energy photons. Because of these emission mechanisms, blazars are characterized by strong radio, X-ray, and γ -ray radiations as well as high polarization and variation across the entire SED. Since blazars dominate the γ -ray sky at high Galactic latitudes, the *Fermi* all-sky survey is expected to shed new light on this relatively rare and poorly understood population.

An investigation of blazar radiation mechanisms (hence the intrinsic SED) is important not only for revealing the nature of blazars themselves, but also for measuring the extragalactic

¹Graduate School of Science, Nagoya University, Furo-cho, Chikusa-ku, Nagoya 464-8602, Japan; matsuoka@a.phys.nagoya-u.ac.jp

²Institute of Astronomy, The University of Tokyo, Osawa 2-21-1, Mitaka, Tokyo 181-0015, Japan

background light (EBL). Since high-energy photons from blazars interact with optical to near-infrared (IR) EBL in the intergalactic space, observations of distant blazars can be used to infer the EBL spectrum if the intrinsic blazar SED is precisely known. With this indirect method, Aharonian et al. (2006) obtained the significantly-lower upper limits of near-IR EBL than those derived from the direct measurements by, e.g., Matsumoto et al. (2005). Recently Matsuoka et al. (2011) succeeded in a direct measurement of optical EBL by re-analyzing the *Pioneer 10/11* data, which is on the smooth extension of the near-IR upper limits obtained by Aharonian et al. (2006).

In this paper, we present the results of our near-IR follow-up observation program of γ -ray blazars and unidentified sources in 1FGL. Despite of the wealth of information there, near-IR wavelength of the whole AGN population is still poorly understood (e.g., Matsuoka et al. 2007, 2008, 2012). We aim to quantify the most distinct features of blazars in near-IR wavelengths, i.e., polarization and variation, in part as a benchmark for future observations. At the same time, we explore the nature of 1FGL unidentified sources by comparing their near-IR properties to the known γ -ray blazars. Dominance of blazars in the γ -ray sky implies that some of the unidentified sources at high Galactic latitudes are similar objects missed in the past surveys at other wavelengths. Revealing the origin of these unidentified γ -ray emissions is of greatest importance, therefore many follow-up studies are being dedicated to this subject (e.g., Ackermann et al. 2011b). We aim to provide complementary information to these follow-up programs from a near-IR view point.

While the second *Fermi*-LAT catalog (2FGL; Nolan et al. 2012) has already been released, this paper is based on 1FGL for consistency with the sample selection of presented observations. We discuss the new 2FGL identifications of the sample later. Magnitudes are presented on the Vega-based system throughout this paper.

2. Observations and Reduction

The sample consists of blazars and unidentified sources extracted from 1FGL. We selected targets at high Galactic latitudes ($|b| > 20^\circ$), with small

position errors (< 5 arcmin with 95-% confidence in most cases), and with bright Two Micron All Sky Survey (2MASS¹) magnitudes ($H_{2\text{MASS}} < 15$ mag) for the blazars whose accurate coordinates are known. The objects listed in the *Fermi*-LAT first AGN catalog (1LAC; Abdo et al. 2010b) were removed from the sample of unidentified sources. The polarimetric observations were performed with the Infrared Survey Facility (IRSF) 1.4-m telescope at the South Africa Astronomical Observatory, Sutherland. We used the near-IR imaging camera SIRIUS (Simultaneous Infrared Imager for Unbiased Survey; Nagashima et al. 1999; Nagayama et al. 2003) which is equipped with three 1024×1024 HgCdTe arrays with the pixel scale of $0''.453$. It was designed to obtain $7'.7 \times 7'.7$ images in the three bands, J ($1.25 \mu\text{m}$), H ($1.63 \mu\text{m}$) and K_s ($2.14 \mu\text{m}$), simultaneously. The instrument provides polarimetric capability called SIRPOL, with an achromatic ($1\text{--}2.5 \mu\text{m}$) wave-plate rotator unit and a polarizer. Source fluxes (F_{000} , F_{225} , F_{450} , F_{675}) in the four wave-plate angles, $0^\circ.0$, $22^\circ.5$, $45^\circ.0$, $67^\circ.5$, are measured in consecutive exposures. The uncertainty of a measured polarization degree is estimated to be less than 0.3% (Kandori et al. 2006).

We summarize the observed targets in Table 1 (for blazars) and 2 (for unidentified sources). The observations were carried out in 2010 December and 2011 February. Mean total exposure times were 30 min for a blazar and 60 min for an unidentified source, divided into single exposures of 20 sec between which the telescope pointing was dithered by 20 arcsec. Typical seeing during the observations was $\sim 1''.4$. Dark and twilight-flat images were obtained before and/or after each night of observations.

Data reduction was performed in a standard manner with a dedicated package SIRPOL of the Image Reduction and Analysis Facility (IRAF²), including dark subtraction, flat fielding, and sub-

¹ This publication makes use of data products from the Two Micron All Sky Survey, which is a joint project of the University of Massachusetts and the Infrared Processing and Analysis Center/California Institute of Technology, funded by the National Aeronautics and Space Administration and the National Science Foundation.

² IRAF is distributed by the National Optical Astronomy Observatory, which is operated by the Association of Universities for Research in Astronomy (AURA) under cooperative agreement with the National Science Foundation.

Table 1: Observation journal of blazars

1FGL ID	Associated blazar	Obs. date ^a	$H_{2\text{MASS}}$ (mag)	H_{IRSF} (mag)	$H_{\text{IRSF}}^{\text{lim}}$ (mag) ²	Polarization (%)
J0021.7–2556	CRATES J0021–2550	Dec 07	14.05 ± 0.03	15.06 ± 0.02	15.54	13.8 ± 2.2
J0033.5–1921	RBS 76	Dec 13	14.08 ± 0.03	14.18 ± 0.01	14.86	6.8 ± 1.8
J0038.4–2504	PKS 0035–252	Dec 13	13.12 ± 0.03	15.92 ± 0.07	14.84	...
J0050.6–0928	PKS 0048–09	Dec 08	13.60 ± 0.03	13.17 ± 0.01	15.65	15.5 ± 0.5
J0120.5–2700	PKS 0118–272	Dec 08	13.40 ± 0.03	13.38 ± 0.01	15.57	6.5 ± 0.6
J0132.6–1655	PKS 0130–17	Dec 08	14.26 ± 0.05	14.90 ± 0.01	15.44	6.4 ± 1.9
J0209.3–5229	BZB J0209–5229	Dec 09	13.80 ± 0.04	14.38 ± 0.01	15.95	3.6 ± 1.0
J0210.6–5101	PKS 0208–512	Dec 07	12.86 ± 0.02	14.64 ± 0.01	15.66	11.6 ± 1.4
J0238.6–3117	BZB J0238–3116	Dec 09	14.43 ± 0.06	14.36 ± 0.01	16.01	3.5 ± 0.9
J0303.5–2406	PKS 0301–243	Dec 07	13.69 ± 0.04	13.17 ± 0.01	15.51	3.6 ± 0.5
J0325.9–1649	RBS 421	Dec 08	14.46 ± 0.04	14.78 ± 0.01	15.41	3.2 ± 1.8
J0334.4–3727	CRATES J0334–3725	Dec 07	14.00 ± 0.03	13.36 ± 0.01	15.35	4.3 ± 0.7
J0423.2–0118	PKS 0420–01	Dec 07	14.53 ± 0.05	15.48 ± 0.02	15.57	8.8 ± 3.0
J0449.5–4350	PKS 0447–439	Dec 07	13.20 ± 0.03	11.87 ± 0.01	15.23	4.5 ± 0.3
J0455.6–4618	PKS 0454–46	Dec 11	14.82 ± 0.05	15.62 ± 0.03	15.43	11.7 ± 3.9
J0522.8–3632	PKS 0521–36	Dec 12	12.21 ± 0.04	12.02 ± 0.01	14.95	10.9 ± 0.4
J0538.8–4404	PKS 0537–441	Dec 12	12.38 ± 0.03	11.72 ± 0.01	15.24	12.8 ± 0.3
J0953.0–0838	CRATES J0953–0840	Dec 09	14.18 ± 0.04	14.39 ± 0.01	15.35	< 3.8
J1022.8–0115	BZB J1022–0113	Dec 12	14.92 ± 0.07	15.41 ± 0.02	15.89	< 3.7
J1059.3–1132	PKS B1056–113	Dec 23	14.80 ± 0.05	13.85 ± 0.01	15.57	11.6 ± 0.8
J1126.8–1854	PKS 1124–186	Dec 23	13.30 ± 0.03	13.57 ± 0.01	15.28	12.6 ± 0.8
J1204.3–0714	CRATES J1204–0710	Feb 14	14.12 ± 0.09	13.85 ± 0.01	16.12	3.0 ± 0.7
J2158.8–3013	PKS 2155–304	Dec 13	10.76 ± 0.03	10.46 ± 0.01	14.04	3.7 ± 0.3
J2222.5–5218	BZB J2221–5225	Dec 13	14.92 ± 0.09	14.40 ± 0.01	15.09	9.2 ± 1.8
J2235.7–4817	PKS 2232–488	Dec 08	12.95 ± 0.03	15.47 ± 0.03	15.43	< 5.8
J2359.0–3035	1H 2351–315	Dec 13	14.72 ± 0.07	14.33 ± 0.01	15.23	1.8 ± 1.5

^aThe observations were carried out from 2010 December to 2011 February.^blimiting magnitudes below which photometry error in a single wave-plate image is less than 0.05 mag.

Table 2: Observation journal of unidentified sources

1FGL ID	Obs. date ^a	$H_{\text{IRSF}}^{\text{lim}}$ (mag) ^b
J0001.9–4158	Dec 26	15.58
J0028.9–7028	Dec 27	15.12
J0032.7–5519	Dec 25	15.67
J0101.0–6423	Dec 27	15.68
J0136.3–2220	Dec 13	15.29
J0143.9–5845	Dec 23, Feb 07	15.95
J0223.0–1118	Feb 13	16.16
J0247.4–6003	Dec 09, Feb 06	16.21
J0311.3–0922	Dec 24	15.67
J0316.3–6438	Dec 23, Feb 11	15.96
J0335.5–4501	Dec 26	16.16
J0345.2–2355	Dec 24	15.86
J0404.5–0850	Dec 22	15.44
J0409.9–0357	Dec 25, Feb 11	15.84
J0439.6–0538	Dec 24	15.71
J0439.8–1857	Dec 24, Feb 06	15.84
J0515.6–4404	Dec 22	15.68
J0523.5–2529	Feb 07	16.67
J0614.1–3328	Feb 07	16.61
J0828.9+0901	Feb 13	16.34
J1101.3+1009	Feb 07	16.73
J1119.9–2205	Feb 06	16.45
J1124.4–3654	Feb 14	16.12
J1141.8–1403	Feb 11	16.65
J1223.4–3034	Feb 13	16.72
J1231.1–1410	Feb 06	16.59
J1311.7–3429	Feb 14	16.15
J1312.6+0048	Feb 11	16.39
J1315.6–0729	Feb 11	16.75
J1351.8–1523	Feb 06	16.71
J1511.8–0513	Feb 06	16.67
J2118.3–3237	Dec 25	15.20
J2152.4–7532	Dec 25	15.53
J2227.4–7804	Dec 28	15.33
J2228.5–1633	Dec 29	14.93
J2241.9–5236	Dec 25	15.39
J2251.2–4928	Dec 29	14.97
J2330.3–4745	Dec 28	15.58
J2355.9–6613	Dec 28	16.07

^aThe observations were carried out from 2010 December to 2011 February.

^b Limiting magnitudes below which photometry error in a single wave-plate image is less than 0.05 mag.

stituting bad pixels. Photometric calibration was achieved by referring to several 2MASS sources within each observed field. While simultaneous J , H , and K_s band images were obtained, we use H -band images in this study because of their highest quality (signal-to-noise ratios). We show an example of a reduced H -band image in the left panel of Figure 1.

We used the *Source Extractor* (Bertin & Arnouts 1996), version 2.5, for aperture photometry of detected sources. Aperture sizes were determined as twice the mean full widths at half maximum of stellar profiles in each image. We required photometry errors to be less than 0.05 mag for polarization measurements, which defines our limiting magnitudes $H_{\text{IRSF}}^{\text{lim}}$ listed in Table 1 and 2. The average values are $H_{\text{IRSF}}^{\text{lim}} = 15.4$ and 16.0 mag for the fields of blazars and unidentified sources, respectively. Polarization degree P_{raw} was then calculated from measured fluxes F_{000} , F_{225} , F_{450} , F_{675} as follows:

$$\begin{aligned}
Q &= F_{000} - F_{450}, \\
U &= F_{225} - F_{675}, \\
I &= (F_{000} + F_{450} + F_{225} + F_{675})/2, \\
P_{\text{raw}} &= 100 \times \frac{\sqrt{Q^2 + U^2}}{I}.
\end{aligned}$$

Here Q and U are the Stokes parameters and I is total intensity. A source with strong polarization stands out in Q/I or U/I images as demonstrated in the right panel of Figure 1.

Since F_{000} , F_{225} , F_{450} , F_{675} are not observed simultaneously, temporal variation of the atmospheric condition causes additional polarimetry errors to those from the standard sky background noise. Hence we estimated polarization error ΔP in a given field from the median P_{raw} value of all the detected sources, assuming that most of those sources at high Galactic latitudes have no intrinsic polarization. Then *true* polarization degrees were derived by de-biasing measured P_{raw} (Wardle & Kronberg 1974) following

$$P = \sqrt{P_{\text{raw}}^2 - \Delta P^2}.$$

Thus the presented values of polarization and its error should be regarded as the lower and upper limits, respectively, considering the above assumption on no intrinsic polarization for most of the

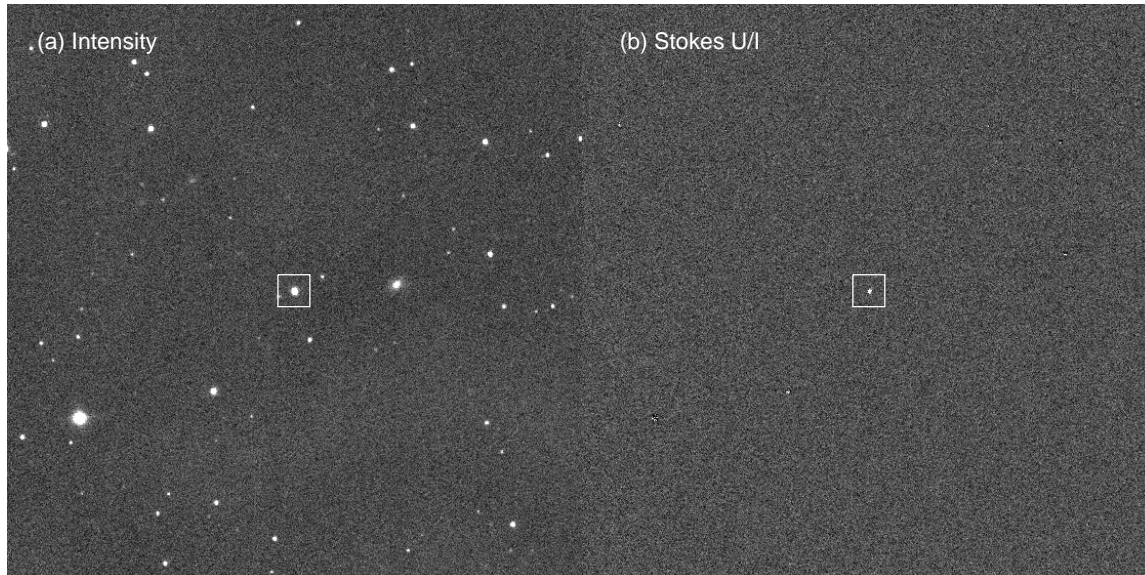


Fig. 1.— IRSF/SIRPOL H -band image of intensity (panel a) and Stokes U/I (b) of a field around the blazar 1FGL J0538.8–4404. The blazar is marked with the boxes.

detected sources. We provide upper limits of polarization for objects with $P_{\text{raw}} < \Delta P$ or $P < \Delta P$.

3. Results and Discussion

We present the results of photometry and polarimetry measurements for the blazars in Table 1. Their polarization and variation since 2MASS observations, as well as those for all other sources detected in the blazar fields, are plotted in Figure 2. Strong variability of the blazars is evident; 22 out of 26 blazars (85 %) have $|H_{\text{IRSF}} - H_{2\text{MASS}}| > 0.25$ mag while only one of the other detected sources shows such variation (~ 0.3 mag; it is likely a contaminating normal star). The blazars are also characterized by pronounced polarization; 10 out of 25 blazars (40 %; polarization was not measured for a blazar associated to J0038.4–2504 due to a large (> 0.05 mag) photometry error) have $P > 10$ %, while all other types of objects are much less polarized. The presented fraction, 40 %, represents a useful benchmark for planning future optical/near-IR polarization follow-up programs of γ -ray selected blazars.

From the above results, we can derive an expected number of blazars which should be discovered by their high polarization and/or variation in the fields of unidentified sources *if they are similar*

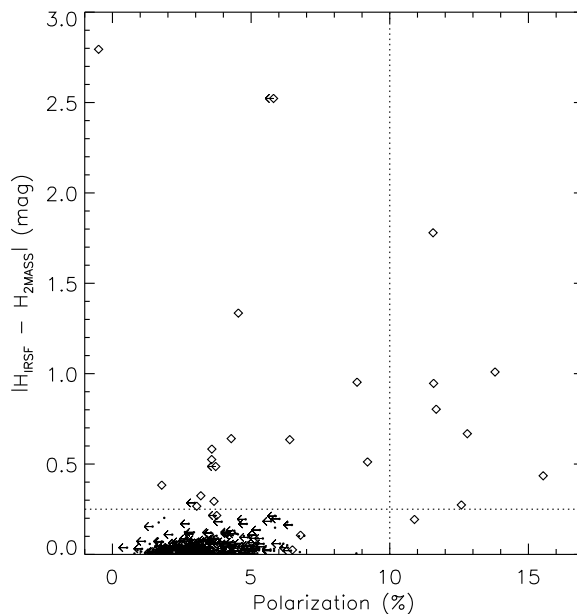


Fig. 2.— Polarization and variation of 326 sources detected in the blazar fields. The diamonds represent the blazars associated to 1FGL sources while the dots represent all other objects. The arrows denote upper limits of polarization.

but unknown blazars. In total, 23 out of 26 blazars (88 %) have pronounced polarization ($P > 10$ %) or variation ($|H_{\text{IRSF}} - H_{2\text{MASS}}| > 0.25$ mag). Since 39 unidentified sources were observed, we would have ~ 35 objects with such distinguishable properties under the above assumption. However, ~ 35 % of them would be fainter than our limiting magnitude $H_{\text{IRSF}}^{\text{lim}} \simeq 16.0$ mag based on the 2MASS magnitude distribution of 1FGL blazars. Furthermore, ~ 32 % of them would be outside SIRPOL field-of-view ($7'.7 \times 7'.7$ arcmin²) when γ -ray positions are used as the telescope pointing center, based on the distribution of distance between γ -ray positions and associated blazars. Considering these restrictions, we expect to find 15 blazars out of 39 fields of unidentified sources if their γ -ray is indeed emitted by a similar population to 1FGL blazars.

Figure 3 shows polarization and variation of 608 objects detected in all the fields of unidentified sources. While three objects are found to have high variation ($|H_{\text{IRSF}} - H_{2\text{MASS}}| > 0.25$ mag), two of them with $P < 7$ % and $|H_{\text{IRSF}} - H_{2\text{MASS}}| \sim 0.3$ mag are likely contaminations; it is consistent with one contamination out of 326 objects in the blazar fields (Figure 2). On the other hand, the object at $P \sim 9$ % and $|H_{\text{IRSF}} - H_{2\text{MASS}}| \sim 1.2$ mag is a promising candidate of new γ -ray blazars. It is found in J1315.6–0729 field, at R.A. $13^{\text{h}}15^{\text{m}}52^{\text{s}}.98$, Dec. $-07^{\circ}33'01''.99$ (J2000.0) with H -band brightness $H_{\text{IRSF}} = 14.1$ mag and $H_{2\text{MASS}} = 15.3$ mag. Its counterparts are found in the NED³; the optical variable source PQV1 J131553.00–073302.0 (Bauer et al. 2009) and the radio source NVSS J131552–073301. We plan to carry out a spectroscopic follow-up observation of this object in the near future.

Except for the above blazar candidate, we found no clear sign of variable or polarized objects in the fields of unidentified sources. The apparent inconsistency between the expected number of blazar candidates as estimated above (15) and the actual number (1) indicates that γ -ray emission of the unidentified sources arises from other types of objects than known 1FGL blazars. They could be non-blazar active galaxies, star-

burst galaxies, or Galactic objects such as pulsars and supernova remnants at relatively high Galactic latitudes, as well as active galaxies with jets but without strong polarization and variability at near-IR wavelengths. In this regard, it is noteworthy that some of them are already identified (or associated) in the latest 2FGL catalog and the *Fermi*-LAT second AGN catalog (2LAC; Ackermann et al. 2011a) as summarized in Table 3. Many of them are pulsars, which is consistent with our observation results. While J2330.3–4745 is associated to the blazar PKS 2326–477, their separation is relatively large and the blazar is outside the field-of-view of our SIRPOL observation.

We are grateful to the IRSF team at Nagoya University, Kyoto University, and National Astronomical Observatory of Japan for great assistance provided during the observations. This work was supported by Grant-in-Aid for Young Scientists (22684005) and the Global COE Program of Nagoya University "Quest for Fundamental Principles in the Universe" from JSPS and MEXT of Japan.

REFERENCES

- Abdo, A. A., Ackermann, M., Ajello, M., et al. 2010, *ApJS*, 188, 405
- Abdo, A. A., Ackermann, M., Ajello, M., et al. 2010b, *ApJ*, 715, 429
- Ackermann, M., Ajello, M., Allafort, A., et al. 2011a, *ApJ*, 743, 171
- Ackermann, M., Ajello, M., Allafort, A., et al. 2011b, *arXiv:1108.1202*
- Aharonian, F., Akhperjanian, A. G., Bazer-Bachi, A. R., et al. 2006, *Nature*, 440, 1018
- Bauer, A., Baltay, C., Coppi, P., et al. 2009, *ApJ*, 705, 46
- Bertin, E., & Arnouts, S. 1996, *A&AS*, 117, 393
- Heidt, J., & Nilsson, K. 2011, *A&A*, 529, A162
- Kandori, R., Kusakabe, N., Tamura, M., et al. 2006, *Proc. SPIE*, 6269,
- Kovalev, Y. Y. 2009, *ApJ*, 707, L56

³ The NASA/IPAC Extragalactic Database (NED) is operated by the Jet Propulsion Laboratory, California Institute of Technology, under contract with the National Aeronautics and Space Administration.

Table 3: 2FGL identification (association) of 1FGL "unidentified" sources in our sample

1FGL ID	Associated source	Object type
J0001.9–4158	1RXS J000135.5–41551	active galaxy of uncertain type
J0101.0–6423	PSR J0101–6422	pulsar
J0223.0–1118	1RXS J022314.6–11174	active galaxy of uncertain type
J0335.5–4501	1RXS J033514.5–44592	active galaxy of uncertain type
J0614.1–3328	PSR J0614–3330	pulsar
J1124.4–3654	PSR J1124–36	pulsar
J1141.8–1403	1RXS J114142.2–14075	active galaxy of uncertain type
J1231.1–1410	PSR J1231–1411	pulsar
J1312.6+0048	PSR J1312+00	pulsar
J2241.9–5236	PSR J2241–5236	pulsar
J2330.3–4745	PKS 2326–477	blazar

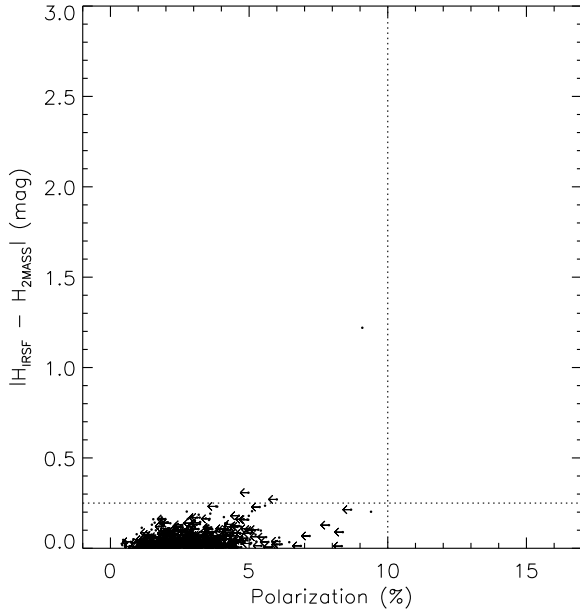


Fig. 3.— Same as Figure 2, but for the fields of unidentified sources.

Matsumoto, T., Matsuura, S., Murakami, H., et al. 2005, ApJ, 626, 31

Matsuoka, Y., Ienaka, N., Kawara, K., & Oyabu, S. 2011, ApJ, 736, 119

Matsuoka, Y., Kawara, K., & Oyabu, S. 2008, ApJ, 673, 62

Matsuoka, Y., Oyabu, S., Tsuzuki, Y., & Kawara, K. 2007, ApJ, 663, 781

Matsuoka, Y., Yuan, F.-T., Takeuchi, Y., & Yanagisawa, K. 2012, PASJ, 64, 44

Nagashima, C., Nagayama, T., Nakajima, Y., et al. 1999, Star Formation 1999, 397

Nagayama, T., Nagashima, C., Nakajima, Y., et al. 2003, Proc. SPIE, 4841, 459

Nolan, P. L., et al., arXiv:1108.1435

Scarpa, R., & Falomo, R. 1997, A&A, 325, 109

The Fermi-LAT Collaboration 2011, arXiv:1108.1435

Wardle, J. F. C., & Kronberg, P. P. 1974, ApJ, 194, 249